

REDISTRIBUTION OF MOMENTS AT CRACKING— THE KEY TO SIMPLER TORSION DESIGN?

By MICHAEL P. COLLINS and PAUL LAMPERT

When a reinforced concrete structure cracks the ratio of torsional to flexural stiffness of its members will drop. The resulting redistribution of torsion and bending moments is the subject of this paper.

Six full scale tests, illustrating this effect for a two beam structure (floor beam-spandrel beam), T-shaped in plan are described. The observed redistribution for different values of such parameters as spandrel beam stiffness, percentage of reinforcement and span length is shown to be well predicted by using the cracked stiffness values.

Further it is shown that specimens designed by assuming zero torsional stiffness for the spandrel beam behaved as satisfactorily as specimens designed by following the conventional procedure of using the uncracked stiffness values.

Keywords: *beams (supports); bending moments; compatibility methods; cracking (fracturing); flexural strength; frames; reinforced concrete; reinforcing steels; stiffness; structural analysis; torsion.*

□ In discussing the design of reinforced concrete to resist torsional loads it is helpful to distinguish between two different types of torsion, one arising from equilibrium requirements and the other needed to satisfy compatibility. We will define these two types in the following manner:

Equilibrium torsion: A torsion is required to maintain equilibrium in the structure.

Compatibility torsion: A twist is required to maintain compatibility in the structure.

In statically determinate structures, only equilibrium torsion exists, while in indeterminate structures both types are possible. A given load produces compatibility torsion in an indeterminate structure if the torsion can be eliminated by releasing redundant restraints. Fig. 11-1 gives examples of both types of torque for a number of typical structures.

In designing a member subjected to equilibrium torsion, it is necessary to provide enough reinforcement to ensure that the member is capable of resisting the full torsion required by statics. Adequate design rules, based on a large amount of recent research, are now available¹ which enable the engineer to proportion his reinforcement for this case.

The method of design for members subjected to compatibility torsion is not so obvious. As what is required from the members is a twist not a torque, the magnitude of the torsion will depend on the value of the torsional stiffness. If

MICHAEL P. COLLINS is an associate professor of civil engineering at the University of Toronto, Canada. He is currently a member of ACI Committee 115, Current Research and ACI Committee 438, Torsion.

ACI member PAUL LAMPERT served as an assistant professor of civil engineering at the University of Toronto, Canada. Dr. Lampert directed the research program "Torsion-Bending-Shear in Reinforced Concrete" at the Institute of Structural Engineering, SFIT Zurich, and was involved in the revision of the CEB torsion provisions in 1969.

the conventional approach of assuming gross stiffness values in the analysis is used unrealistically large torsions will result. If under load the member does not crack the torsional reinforcement provided will be virtually unstressed. If, on the other hand, the member cracks, its torsional stiffness will be substantially reduced² and the resulting redistribution of loads will reduce the torsion in the member and hence the need for torsional reinforcement.

If instead of using gross torsional stiffness values it was assumed that the torsional stiffness was zero very simple design procedures, for the case of compatibility torsion, would result. This assumption would lead to zero values for the torsion and hence only minimum torsional steel (needed to ensure ductility and limit cracks) would have to be provided.

The feasibility of such a procedure for the case of a simple structure, is examined in this paper.

ANALYSIS OF THE STRUCTURE TESTED

The two beam structure (floor beam-spandrel beam) shown in Fig. 11-2, was chosen for study. In this structure the spandrel beam is subjected to compatibility torsion. This torsion will restrain the floor beam, resulting in the distribution of moments labelled "Method A" in Fig. 11-3.

Analysis of the structure reveals that the magnitude of the restraining moment (X) is given by

$$\frac{X}{PL_F} = \frac{3 \cdot \frac{1}{2} \left(\frac{L_S}{L_F} \right)^3 \frac{EI_F}{EI_S}}{16 + \left(\frac{L_S}{L_F} \right)^3 \frac{EI_F}{EI_S} + 12 \frac{L_S}{L_F} \frac{EI_F}{GK_S}} \quad (1)$$

where EI_F and EI_S are the flexural stiffnesses of the floor and the spandrel, and GK_S is the torsional stiffness of the spandrel.

It can be seen that if the spandrel is infinitely stiff ($EI_S = \infty$, $GK_S = \infty$) the restraining moment is $3PL_F/16$, the value for a propped cantilever. On the other hand, if the spandrel beam has zero torsional stiffness, the restraining moment is zero. The distribution in this case is labelled "Method B" in Fig. 11-3.

DESIGN AND TESTING OF THE SPECIMENS

Specimen S1 (see Table 11-1) was the basic test specimen. It had a 15 ft floor beam and a 9 ft 6 in. spandrel beam, both 10.2 x 17 in. in cross-section, and was designed for a load of about 40 kips in the midspan of the floor beam. The reinforcement was proportioned in the conventional manner, here called method A. That is gross stiffness values were used to determine the moments and torques which in turn determined the amount of reinforcement required to satisfy the code.¹

Specimen S2 had the same external dimensions as S1 and was designed to resist approximately the same load. However, S2 was designed by assuming zero torsional stiffness (method B) and providing only a minimum amount of torsional steel. This resulted in S2 having slightly more steel in the floor beam (174 lb-152 lb) but considerably less steel in the spandrel beam (68 lb-137 lb). Specimens S3 and S4 both had stiffer spandrel beams (17 x 17 in.) and hence different values of the ratios EI_F/EI_S and EI_F/GK_S . Specimen S3 was designed by method A for a load of 52 kips, while S4 was designed for a load of 43 kips by method B.

Specimen S6 also had a design load near 40 kips but had a different value for the length ratio (L_S/L_F). Specimen S5 had identical reinforcement to S6 but its length ratio was the same as for S1 - S4.

Fig. 11-4 indicates, diagrammatically, the loading system and the instrumentation used in the tests. The ends of the spandrel beam were "torsionally restrained" by means of hydraulic jacks pulling on outrigger arms. Load cells on the pull rods enabled the torsion, which was needed to keep the ends of the spandrel level, to be measured accurately. The twist of the spandrel, deflection of the spandrel and the floor beam, steel strains, concrete strains and crack widths were all measured and are given in detail elsewhere.³ An overall view of a specimen under test is shown in Fig. 11-5.

GENERAL BEHAVIOR OF THE SPECIMENS

The general behavior of the specimens is best described by referring to the load-deflection diagrams (Fig. 11-6, 11-7, and 11-8). It will be seen that as far as deflections are concerned, the behavior of specimens S1 and S2 is remarkably similar (Fig. 11-6). For the specimen designed on the assumption of zero torsion (S2) first yielding occurs at a higher load than for S1 while failure occurs at a

slightly lower load. In both cases the final failure was due to crushing of the concrete compression zone under the load.

Specimens S3 (conventional design) and S4 (zero torsion), having different design loads, did not exhibit such similar behavior (Fig. 11-7). After yielding of the longitudinal steel in the floor beam, the load on S3 rose considerably. This load finally resulted in a failure of the joint. Specimen S4, on the other hand, showed only a small increase in load after first yielding and experienced no difficulties with either the shear capacity of the floor beam or the integrity of the joint.

The behavior of S5 (Fig. 11-8) was similar to S2 except that yielding and failure occurred at lower loads, while because of excessive longitudinal spandrel steel, yielding of this steel occurred at a late stage. Specimen S6 exhibited the usual sequence of steel yielding but failed by a loss of shear capacity at the joint.

The load-deflection curves of Fig. 11-8 also indicate the effect of the ratio of spandrel beam length, L_S , to floor beam length, L_F , on the behavior of the specimens. The deflection under the load, Δ_1 , is much greater than the deflection under the joint, Δ_2 , for specimen S5 ($L_S/L_F = 0.63$), but for S6 ($L_S/L_F = 1.58$) these two deflections are almost equal. As the twist of the spandrel will be a function of the difference between these deflections, this indicates that the torsion in S6 will be very small.

An overall view of four of the specimens (S1-S4) after failure is given in Fig. 11-9. The similarity in appearance of S1 and S2 (the lower two specimens) will be noted. Evidence of the shear failure and the joint failure in specimen S3 and of the concrete crushing in the other three specimens can be seen.

BEHAVIOR OF THE JOINT

The joint between the floor beam and the spandrel beam was the cause of final failure in two of the six specimens (S3 and S6). Great care had been taken in detailing these joints. In accordance with recommendations for indirect support,⁴ closely spaced spandrel stirrups were provided through the joint to "hang-up" 100 percent of the arriving load. Further, the bottom longitudinal bars of the floor beam (the load-bringer) were placed on top of the bottom longitudinal bars of the spandrel beam (the load-carrier). In spite of this care, some joints failed, as the photos taken before and after spalling of S3 vividly show (Fig. 11-10).

At the joint, the floor beam is subjected to a negative moment as well as a shear in the manner analogous to the support region of a continuous beam. Flexure-shear cracks penetrate far into the compression zone of the beam (see Fig. 11-10). The compression diagonals between these cracks push strongly upon the bottom longitudinal steel of the floor beam. Unlike the support of a continuous beam, there are here no vertical compressive stresses to help the bar resist the push. In fact, as the spandrel is in positive bending, there are lateral tensile stresses that further weaken the joint. While provisions had been made for "hanging-up" the load in the spandrel only the usual shear reinforcement had

been provided in the floor beam. That this proved inadequate to resist the push on the longitudinal steel can be seen clearly from the post-spalling photo in Fig. 11-10. It might be added that failure to place the floor beam steel on top of the spandrel beam would have enabled the bars to push-out at a much lower load.

It would appear to be sound practice to provide the floor beam with closely spaced stirrups in the region close to the joint capable of "hanging-up" 100 percent of the load. Because the location of the critical compression diagonals is largely a matter of chance, it would still be wise to provide spandrel stirrups capable of "hanging-up" 100 percent of the load.

CRACKING BEHAVIOR

As well as providing adequate strength, the reinforcement must control the crack widths at working loads. It might thus be suspected that providing less torsional steel will lead to wider torsional cracks.

The photos in Fig. 11-11 show specimens S1 and S2, at a load corresponding to the maximum feasible working load and at ultimate load. It will be observed that there is no significant difference in the crack patterns at working load, but that at ultimate the cracks in S1 are more closely spaced.

A plot of the maximum crack widths confirms this trend (Fig. 11-12). Up till a load of about 30 kips both specimens have similar crack widths, whereas beyond this load S2 (the specimen with less steel) has wider cracks. A similar behavior is also shown by S3 and S4 except that in this case, the deviation between the two specimens is much smaller.

TORSION MEASURED IN THE SPANDREL BEAMS

Of prime interest in our investigation is the magnitude of the "compatibility torsion" caused by the twist of the spandrel beams.

The measured twists of the spandrel for specimens S1 and S2, plotted as a function of the applied load, are given in Fig. 11-13. Once again the remarkably similar behavior of these two specimens will be noted. Apparently the additional spandrel steel in S1 has very little effect on the magnitude of the twist. The same trend is apparent in Fig. 11-14 where it can be seen that the specimen designed for zero torsion (S4) in general suffers less twist than the conventionally designed specimen.

While the twists in S1 and S2 are similar, the torques are not. The torque-twist curves show (Fig. 11-15) that as expected the spandrel with more steel (S1) has a higher torque for the same twist.

The torsion in the spandrel can also be studied in terms of the restraining moment, X , on the floor beam. Fig. 11-16 shows the measured values of this moment for S1 and S2 as a function of the applied load. If the stiffness values are known, X can be predicted from Eq. (1). The prediction obtained by using gross stiffness values is labelled "Gross" in Fig. 11-16 (see Table 11-2). It can be

seen that after cracking the restraining moments are considerably less than those predicted by the gross analysis, with the moments in S2 (zero torsion design) being even less than those in S1. Rather than rising linearly with the load the restraining moment, and hence the torque, can be seen to remain almost constant between cracking load and first yielding.

The same pattern of behavior is exhibited by specimens S3 and S4 (Fig. 11-17). This time the conventionally designed specimen, S3, has much higher values of X than the "zero torsion" specimen, S4. These values, however, are still considerably smaller than those predicted by the gross analysis.

The effect of spandrel length on the magnitude of the torsion (torque = $X/2$) can be seen in Fig. 11-18. As indicated in the discussion of deflections, the long spandrel beam of S6 means the torque will be very low. It will be noted that for this specimen torsion cracks did not form until just before failure.

PREDICTED POSTCRACKING STIFFNESS

The A.C.I. Code¹ offers the following guidelines in choosing appropriate design values for stiffness: "Any reasonable assumptions may be adopted for computing the relative flexural and torsional stiffnesses. . . . The assumptions made shall be consistent throughout the analysis." We have seen above that the use of gross stiffness values led to unrealistically high predictions of the postcracking torsion. Perhaps a more "reasonable" approach would be to use the postcracking stiffness values. Methods for calculating the cracked flexural stiffness are well established with the "transformed section" approach being the most widely known. A companion paper in this volume² presents a theoretical derivation and experimental confirmation of an expression for the postcracking torsional stiffness. This expression is:

$$GK_{cr} = \frac{E_s (b_o h_o)^2 A_h}{2 (b_o + h_o) s} (1 + m) \quad (2)$$

Where A_h = cross-sectional area of the hoop bar

b_o, h_o = dimensions between the longitudinal corner bars

s = spacing of the hoops

m = ratio of the volume of longitudinal steel to the volume of hoop steel

and E_s = Young's modulus of the steel.

The stiffness values predicted by Eq. (2) are plotted on the torque-twist curves given in Fig. 11-15. The stiffness, being a function of the amount of hoop steel, is naturally greater for S1 (conventional design) than for S2 (zero torsion). It has been shown² that for a beam in pure torsion Eq. (2) gives a very accurate prediction of the stiffness at first yielding. For the case of the spandrels, the expression under-estimated this torsional stiffness (see Fig. 11-15). The spandrels, being

subjected to torsion, bending and shear, were not uniformly cracked. The regions of low tensile stress remained virtually uncracked, accounting for the additional stiffness of the spandrels.

PREDICTED REDISTRIBUTION AFTER CRACKING

Use of cracked stiffness values will lead to different stiffness ratios and hence to a different prediction of the moment distribution. If Table 11-2 is examined it will be seen that while the flexural stiffness ratio (EI_F/EI_S) is not greatly affected by the change from the "gross" to the "cracked" analysis the ratio of flexural to torsional stiffness (EI_F/GK_S) increases tremendously. This increase means a substantial drop in the predicted magnitude of the torque.

This "drop" can be seen if the "gross" and the "cracked" predictions for the value of the restraining moment (X) are compared (see Fig. 11-16). As might be expected, a larger drop is predicted for specimens with less torsional steel, a prediction verified by the experimental results.

It will be observed (Fig. 11-16, 11-17, and 11-18) that the measured values of X lie between the gross and the cracked predictions. After cracking the experimental curves veer away from the "gross" prediction and head towards the "cracked" prediction. Yielding of the steel again changes the stiffness ratios and may reverse this trend.

To illustrate the predicted and observed moment distributions in a more conventional manner Fig. 11-19 was prepared. In this figure the moments predicted by gross analysis, the moments predicted by cracked analysis, and the measured moments at a load of 40 kips, are compared for specimen S4. (The same comparison could be made in Fig. 11-17). It can be seen from Fig. 11-19 that the analysis using cracked stiffness values leads to a more accurate prediction of the moment distribution than that based on gross stiffness values.

PREDICTED TWIST OF THE SPANDREL—AN INDICATION OF CRACKING BEHAVIOR

One objection to relaxing and simplifying current torsional design procedures would be the suspicion that providing less torsional reinforcement would lead to less satisfactory crack control. Though it was shown above that the crack pattern of specimens designed by the two methods ("conventional" and "zero torsion") did not differ at working loads it might be argued that for other percentages of reinforcement or other frame configurations this would not be the case.

The amount of torsional cracking that will occur in a member will be a function of the amount of twist which the member must undergo. In Fig. 11-20 the measured amount of cracking (expressed as the sum of the crack widths per unit length) is plotted as a function of twist for a number of beams reported in the literature.^{5,6} The beams in this plot were tested in pure torsion, were square in cross-section, had about the same size, and all but one (T4) were hollow. Each

beam had a different distribution or a different amount of reinforcement. It can be seen (Fig. 11-20) that in each case the amount of cracking is nearly a linear function of the twist. It will further be observed that this behavior is not affected by yielding of the reinforcement. It can thus be concluded that the amount of cracking is governed by the twist and is not influenced by the force induced in the reinforcement.

Though the amount of cracking is not influenced by the distribution of the reinforcement the maximum crack width obviously will be. Closely spaced steel will assure a large number of small cracks while wide spacing of the hoops will produce a small number of large cracks (compare S1 and S2 in Fig. 11-11 and 11-12).

The twist of the spandrel, and hence the amount of cracking, can be predicted if the stiffness values are known. Values of the twist obtained by using gross and cracked stiffness values are compared to the experimental values in Fig. 11-13. As might be expected the observed twist before yielding lies between the gross and the cracked predictions. What may be surprising is the fact that the cracked analysis predicts a smaller twist for the beam with less torsional steel (S2). The explanation for this is that the rotation of the joint is predominantly controlled by the flexural behavior of the floor beam. Thus the loss of torsional stiffness incurred by providing less torsional steel is more than compensated for by the additional flexural stiffness generated by providing additional floor beam steel.

To investigate whether other specimens designed by Method B (zero torsion) will also have smaller predicted values of twist (and hence have less cracking), Fig. 11-21 and 11-22 were prepared.

The effect of the percentages of reinforcement on the angle of twist of the spandrel at the design load may be seen in Fig. 11-21. The figure shows that if the assumed frame is designed for a larger load, and hence contains a higher percentage of reinforcement, the predicted angle of twist at the design load will be greater. The figure also predicts that over the whole range of feasible reinforcement, for the section properties assumed, a frame designed by Method B will twist less than one designed for the same load by Method A. (A sample design and calculation is given in detail in Appendix A.) The general trend of the theoretical predictions is confirmed by the three experimental points plotted.

The effect of the ratio of floor beam length to spandrel beam length (L_F/L_S) on the angle of twist of the spandrel is shown in Fig. 11-22. In constructing this figure it was assumed that $L_F + L_S = 24$ ft 6 in. and that the reinforcement in the floor beam for Method B consisted of two #8 bars. These assumptions enabled the results of specimens S5 and S6 to be plotted in the figure. It can be seen that the predicted angle of twist per unit length increases rapidly as the spandrel is shortened, this prediction being confirmed by the experimental points. The figure also shows that over a wide range of length ratios the cracked analysis predicts a smaller angle of twist for the frames designed by Method B than for those designed by Method A. The large values of twist for the very short spandrels (when $L_F/L_S = 4$ the spandrel is only 4.9 ft long, that is only about 25 in. protrudes from each side of the floor beam) indicate that for these frames crack widths may be a problem with either design method.

CONSEQUENCES FOR DESIGN

We have seen that the use of cracked stiffness values in design would be a "reasonable assumption" and would lead to accurate predictions of the torque. However, before the cracked stiffness can be determined, the reinforcement must be designed and to design the reinforcement we must know the magnitude of the torque. The use of cracked stiffness values would thus lead to a cumbersome trial and error design procedure.

The assumption of zero torsional stiffness, on the other hand, would lead to very simple design procedures (compare method A and method B in the appendix). The question then is whether this qualifies as a "reasonable assumption." The behavior of the specimens designed on the basis of this assumption certainly indicates that for these frames the assumption was reasonable. Further, it was shown above that for a wide range of variables, the predicted cracking behavior of specimens designed using this assumption was not significantly different from that of conventionally designed specimens.

A question might be raised about the rotational capacity of the beams. The ability to twist will be exhausted when the limiting shear strain, γ_L , is reached on one face of the beam. Experiments⁶ have shown that the value of γ_L lies between 0.01 and 0.02. Using the lower values for the shear strain we can derive a conservative expression for the twist capacity from Eq. (23) of Reference (2):

$$\zeta_L = 0.01 \frac{b_o + h_o}{b_o h_o} \quad (3)$$

It will be found that this twist capacity is large enough not to be critical. For example, for the specimens investigated in Fig. 11-21 and 11-22, Eq. (3) gives a value of ζ_L of 19.4×10^{-4} rad./in., while the largest twist at design load is 4×10^{-4} rad./in.

It thus appears that for the simple type of frame investigated the assumption of zero torsional stiffness is reasonable. In effect this means that for the case of compatibility torsion we reinforce the spandrel for a twist rather than a torque. Thus not the amount but the distribution of the steel is important. A "minimum amount" of closely spaced longitudinal and web steel will ensure that the member can sustain the twist in a ductile manner without displaying excessive crack widths.

In the case of a very short spandrel beam, we have seen above that crack widths may be a problem with either design method. In such a case it is probably wise to dimension the beam so that under service loads it remains torsionally uncracked.

For structures more complex than the simple frames investigated secondary effects, such as the restraints imposed on the torsional member by adjacent columns and slabs, may affect the validity of the assumption of zero torsional stiffness. Such structures are presently being investigated, in a continuation of this work, at the University of Toronto.

SUMMARY AND CONCLUSION

It was found necessary to draw a distinction between "equilibrium torsion," in which a torsion is required to maintain equilibrium, and "compatibility torsion," in which a twist is required to maintain compatibility. The test results of six floor beam-spandrel beam structures, in which the spandrel was subjected to compatibility torsion, are reported. These results are explained and generalized in a companion theoretical study. The conclusions to be drawn from this work are:

1. In designing for compatibility torsion the magnitude of the torsion at the design load is overestimated if gross stiffness values are used in the analysis.
2. At cracking the ratio of torsional to flexural stiffness will drop causing redistribution of the torsion and the bending moment.
3. The observed redistributions for different values of spandrel beam stiffness, percentage of reinforcement and span length are well predicted by using the cracked stiffness values.
4. Specimens designed by assuming that the members had zero torsional stiffness behaved as satisfactorily as specimens designed by following the conventional procedure of using the uncracked stiffness values.
5. It appears that for the case of compatibility torsion we should design for a twist not a torque. Thus the main function of the "torsional" reinforcement is to distribute the cracks caused by the twist. Additional torsional steel merely increases the torque in the member while having little effect on the twist.
6. Very simple design procedures for compatibility torsion will be feasible when it is demonstrated that for most structures assigning a value of zero to the torsional stiffness is a "reasonable assumption."

For the structure studied experimental and theoretical results show that a substantial redistribution of moments occurred at cracking leading to a significant reduction of the torque. This reduction makes feasible the assumption of zero torsional stiffness and could thus be considered as the key to simpler torsional design.

ACKNOWLEDGMENTS

The investigation reported in this paper was made possible by a grant from the National Research Council of Canada, which is gratefully acknowledged. Thanks are also extended to the Steel Company of Canada Limited and to Lake Ontario Cement Limited for providing the materials needed for the test specimens.

The specimens were manufactured and tested by M. E. Ozerdinc, a Research Assistant in Civil Engineering, with the help of technical personnel and facilities supplied by the Department of Civil Engineering, of the University of Toronto.

APPENDIX A

EXAMPLE OF DESIGN AND ANALYSIS CALCULATIONS

For the member properties given in Fig. 11-21 we will design specimens by the two different methods (A and B) to resist a design load of 40 kips. As we wish to compare the analysis with results from specimens of known dimensions and material properties we will use a capacity reduction factor (ϕ) of 1.0.

DESIGN BY METHOD A

Step 1. Determine gross stiffness values:

Flexural stiffness of floor and spandrel beam

$$EI_F = EI_S = E_c \frac{bh^3}{12} = 3.6 \times 10^3 \times \frac{10.2 \times 17^3}{12} = 15 \times 10^6 \text{ kip. in.}^2$$

Torsional stiffness of the spandrel

$$GK_S = G_c \beta b^3 h = 0.5 \times 3.6 \times 10^3 \times 0.21 \times 10.2^3 \times 17 = 6.8 \times 10^6 \text{ kip. in.}^2$$

where β is the St. Venant stiffness factor.

Step 2. Use stiffness values to determine moments and torques:

From Eq. (1) the restraining moment X equals:

$$\frac{X}{PL_F} = \frac{3 - \frac{1}{2} \left(\frac{L_S}{L_F} \right)^3 \frac{EI_F}{EI_S}}{16 + \left(\frac{L_S}{L_F} \right)^3 \frac{EI_F}{EI_S} + 12 \frac{L_S}{L_F} \frac{EI_F}{GK_S}}$$

In our case $EI_F/EI_S = 1.0$, $EI_F/GK_S = 15/6.8 = 2.2$, $L_S/L_F = 9.5/15 = 0.633$

which gives $\frac{X}{PL_F} = 0.0868$.

From Fig. 11-3 maximum positive moment in the floor beam

$$= \frac{PL_F}{4} - \frac{X}{2} = \frac{PL_F}{2} (0.5 - 0.0868) = 37.2P \text{ kip. in.} = 1490 \text{ kip. in.}$$

Negative moment in the floor beam $= X = 15.6P = 626 \text{ kip. in.}$

Maximum moment in the spandrel

$$= \frac{PL_S}{4} (0.5 + 0.0868) = 16.8P = 672 \text{ kip in.}$$

Torque in the spandrel

$$= \frac{X}{2} = 7.8P = 313 \text{ kip in.}$$

Shear in the spandrel

$$= \frac{P}{4} + \frac{X}{2L_F} = .293P = 11.7 \text{ kips.}$$

Step 3. Design floor beam flexural steel:

$$\text{Positive moment} = 1490 \text{ kip in.} \quad bd^2f'_c = 10.2 \times 16^2 \times 3.5 = 9,130 \text{ kip in.}$$

$$\frac{M}{bd^2f'_c} = .162 = q(1 - 0.59q) \quad \therefore q = 0.182$$

$$\therefore p = q \frac{f'_c}{f_y} = .182 \frac{3.5}{60} = 0.0106; \quad A_S = 1.73 \text{ sq in.}$$

$$\text{Negative moment} = 626 \text{ kip in.} \quad \frac{M}{bd^2f'_c} = .0688$$

$$\therefore q' = .072 \quad \therefore p' = 0.0042 \quad A'_S = 0.68 \text{ sq in.}$$

Step 4. Design spandrel beam flexural steel.

$$\text{Moment} = 672 \text{ kip in.} \quad bd^2f'_c = 9,130 \text{ kip in.}$$

$$\frac{M}{bd^2f'_c} = .0735 \quad \therefore q = 0.077 \quad \therefore p = 0.0045$$

$$A_S = 0.73 \text{ sq in.}$$

Step 5. Design spandrel beam web steel:

$$T = 313 \text{ kip in.}$$

$$V = 11.7 \text{ kips}$$

$$\tau_u = \frac{3T}{x^2y} = \frac{3 \times 313}{10.2^2 \times 17} = 532 \text{ psi}$$

$$v_u = \frac{V}{bd} = \frac{11.7}{10.2 \times 16} = 72 \text{ psi}$$

$$\tau_c = \frac{2.4 \sqrt{f'_c}}{\sqrt{1 + (1.2 v_u / \tau_u)^2}} = 140 \text{ psi}$$

$$v_c = \frac{2 \sqrt{f'_c}}{\sqrt{1 + (\tau_u / 1.2 v_u)^2}} = 19 \text{ psi}$$

$$(\tau_u - \tau_c) = 392 \text{ psi} \quad \text{and} \quad (v_u - v_c) = 53 \text{ psi}$$

Area of web steel for torsion

$$\frac{A_h}{s} = \frac{(\tau_u - \tau_c) x^2 y}{3 \Omega x_1 y_1 f_y} \quad \text{where } \Omega = 0.66 + 0.33 (y_1 / x_1) = 1.25$$

$$= \frac{.392 \times 10.2^2 \times 17}{3 \times 1.25 \times 9 \times 16 \times 40} = 0.032 \text{ sq in./in.}$$

Area of web steel for shear

$$\frac{A_h}{s} = \frac{(v_u - v_c) b}{2 f_y} = \frac{.053 \times 10.2}{2 \times 40} = 0.0068 \text{ sq in.}$$

Step 6. Longitudinal steel for torsion:

$$A = 2 \left(\frac{A_h}{s} \right) (x_1 + y_1) = 2 \times 0.032 (9 + 16) = 1.6 \text{ sq in.}$$

Step 7. Summarize design:

$$\text{Floor beam:} \quad A_S = 1.73 \text{ sq in.} \quad A'_S = 0.68 \text{ sq in.}$$

$$\text{Spandrel beam:} \quad A_S = 0.73 + 0.8 = 1.53 \text{ sq in.} \quad A'_S = 0.8 \text{ sq in.}$$

$$\frac{A_h}{s} = 0.032 + 0.0068 = 0.0388 \text{ sq in./in.}$$

DESIGN BY METHOD B

Step 1. Determine moments:

$$\text{Positive moment in floor beam} = \frac{PL_F}{4} = \frac{40 \times 180}{4} = 1800 \text{ kip in.}$$

$$\text{Moment in spandrel} = \frac{PL_S}{8} = \frac{40 \times 114}{8} = 570 \text{ kip in.}$$

$$\text{Shear in spandrel} = \frac{P}{4} = 10 \text{ kips.}$$

Step 2. Design floor beam flexural steel:

$$\text{Positive moment} = 1800 \text{ kip in.} \quad bd^2f'_c = 9130 \text{ kip in.}$$

$$\frac{M}{bd^2f'_c} = .197 \quad \therefore q = .228 \quad \therefore p = 0.0133 \quad \therefore A_S = 2.17 \text{ sq in.}$$

$$\text{Nominal top steel needed } 2 - \#3 \quad A'_S = 0.22$$

Note: In actual design it may be better practice to place more top steel in the beam to limit flexural cracking.

Step 3. Design spandrel beam flexural steel.

$$\text{Moment} = 570 \text{ kip in.} \quad \frac{M}{bd^2f'_c} = .0624 \quad q = 0.065$$

$$\therefore p = .0038 \quad A_S = 0.62 \text{ sq in.}$$

$$\text{Need nominal top steel } 2 - \#3 \quad A'_S = 0.22 \text{ sq in.}$$

Step 4. Design spandrel beam web steel:

$$V = 10 \text{ kips} \quad v_u = \frac{10}{10.2 \times 16} = 61 \text{ psi}$$

$$v_c = 2 \sqrt{f'_c} = 118 \text{ psi}$$

Use minimum web steel for ductility and crack control.

$$\frac{A_h}{s} = \frac{25b}{f_y} = \frac{25 \times 10.2}{40,000} = 0.0064 \text{ sq in./in.}$$

Step 5. Summarize design:

$$\text{Floor beam:} \quad A_S = 2.17 \text{ sq in.} \quad A'_S = 0.22 \text{ sq in.}$$

$$\text{Spandrel beam:} \quad A_S = 0.62 \text{ sq in.} \quad A'_S = 0.22 \text{ sq in.}$$

$$\frac{A_h}{s} = 0.0064 \text{ sq in./in.}$$

CALCULATION OF THE ANGLE OF TWIST

Now that we have designed the specimens we can predict their angles of twist at a load of 40 kips.

The angle of twist per unit length of the spandrel (ζ) can be found by dividing the torque in the spandrel by the torsional stiffness.

$$\zeta = \frac{X/2}{GK_S}$$

The torque at the design load ($X/2$) can be estimated from Eq. (1) using the cracked values for the stiffnesses. The stiffness values can be found from the section properties by "transformed sections" and Eq. (2). These calculations are summarized in Table 11-A-1 below, where it can be seen that the twist at the design load of the specimen designed by the two methods is about the same (1.46×10^{-4} and 1.37×10^{-4} rad./in.).

TABLE 11-A-1—TWIST AT DESIGN LOAD

Specimen	Cracked Stiffness Values			Torque kip in.	Twist rad/in.
	EI_F kip in. ²	EI_S kip in. ²	GK_S kip in. ²		
Method A	7.7×10^6	6.8×10^6	0.760×10^6	111	1.46×10^{-4}
Method B	8.9×10^6	3.4×10^6	0.175×10^6	24	1.37×10^{-4}

The calculations above enable two points in Fig. 11-21 to be plotted. A large number of similar calculations were made in the preparation of Fig. 11-21 and 11-22.

REFERENCES

1. ACI Committee 318, "Building Code Requirements for Reinforced Concrete (ACI 318-71)," American Concrete Institute, Detroit, 1971, 78 pp.
2. Lampert, Paul, "Postcracking Stiffness of Reinforced Concrete Beams in Torsion and Bending," *Analysis of Structural Systems for Torsion*, SP-35, American Concrete Institute, Detroit, 1972, pp. 384-432.
3. Ozerdinc, M. E.; Lampert, P.; and Collins, M. P., "Torsion-Bending-Redistribution at Cracking—An Experimental Investigation," *Civil Engineering Publication No. 72-23*, University of Toronto, Dec. 1972.

4. Leonhardt, F., "Die verminderte Schubdeckung bei Stahlbetontragwerken," *Der Bauingenieur* (Berlin-Wilmersdorf), V. 40, No. 1, Jan. 1965.
5. Mitchell, D.; Lampert, P.; and Collins, M. P., "The Effect of Stirrup Spacing and Longitudinal Restraint on the Behavior of Reinforced Concrete Beams Subjected to Pure Torsion," *Civil Engineering Publication* No. 71-22, University of Toronto, Oct. 1971.
6. Lampert, Paul, "Torsion und Biegung von Stahlbetonbalken," *Schweizerische Bauzeitung* (Zurich), V. 88, No. 5, Jan. 1970, pp. 85-95.

NOTATION

A_h	= area of one leg of a hoop
A_s	= area of positive flexural steel
A'_s	= area of negative flexural steel
b	= width of member
b_o	= width between longitudinal corner bars
d	= distance from extreme compression fiber to centroid of tension reinforcement
E_c	= modulus of elasticity of concrete
E_s	= modulus of elasticity of steel
EI_F	= flexural stiffness of the floor beam
EI_S	= flexural stiffness of the spandrel beam
f'_c	= compressive strength of the concrete
f_y	= yield strength of the reinforcement
GK_S	= torsional stiffness of the spandrel beam
G_c	= shear modulus of the concrete
h	= overall height of the member
h_o	= height between longitudinal corner bars
L_F	= span of the floor beam
L_S	= span of the spandrel beam
M	= bending moment
m	= ratio of the volume of longitudinal steel to the volume of hoop steel
P	= load applied to the floor beam
p	= A_s/bd
q	= $p f_y/f'_c$
s	= spacing of the hoops

T	= torsion
V	= shear
v_c	= nominal shear stress carried by concrete
v_u	= nominal design shear stress
w	= crack width
X	= restraining moment of the floor beam
x	= shorter overall dimension of the cross-section
x_1	= shorter dimension of the hoop
y	= longer overall dimension of the cross-section
y_1	= longer dimension of the hoop
β	= St. Venant stiffness factor
γ_L	= limiting shear strain
Δ_1	= deflection under the load
Δ_2	= deflection under the joint
ζ	= twist per unit length of the spandrel
ζ_L	= twist capacity of the spandrel
τ_c	= nominal torsional stress carried by concrete
τ_u	= nominal design torsional stress
Ω	= $0.66 + 0.33 (y_1/x_1)$

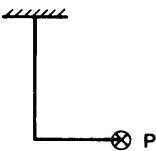
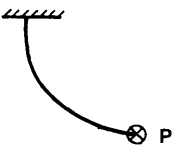
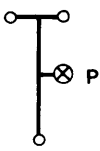
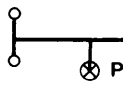
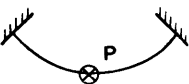
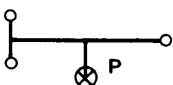
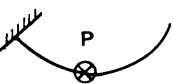


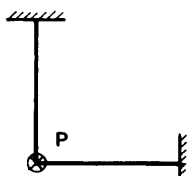
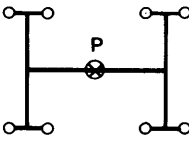
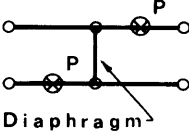
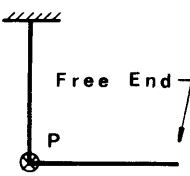
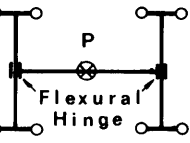
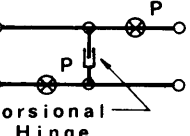
STATICALLY DETERMINATE SYSTEMS			TYPE OF TORSION
			Equilibrium Torsion
STATICALLY INDETERMINATE SYSTEMS			TYPE OF TORSION
Real Systems	Reduced Indeterminacy	Torsional Moment	Equilibrium Torsion
 	 	 	
  	  	Eliminated Eliminated Eliminated	Compatibility Torsion

Fig. 11-1—Equilibrium torsion—compatibility torsion

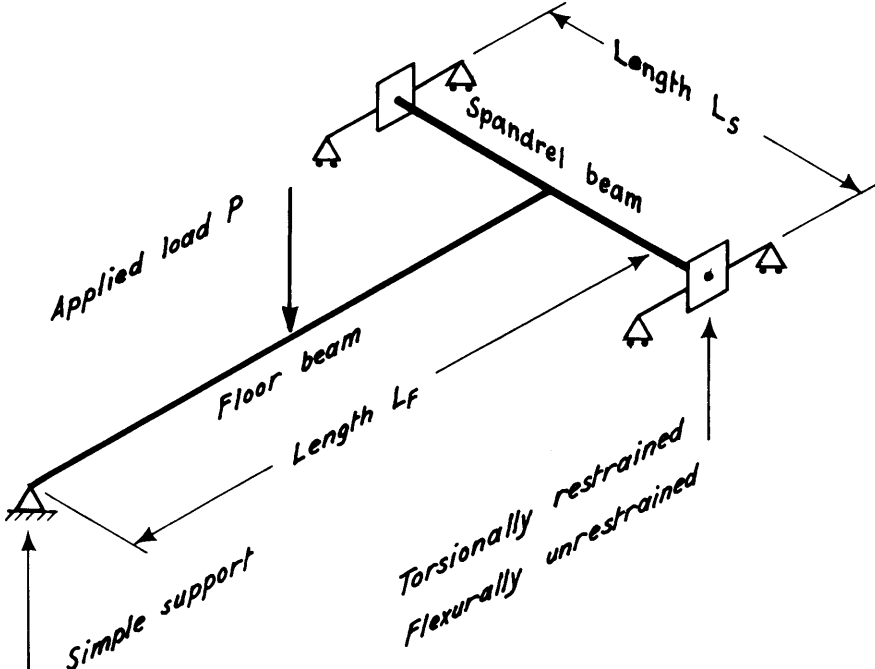


Fig. 11-2—Structural frame investigated

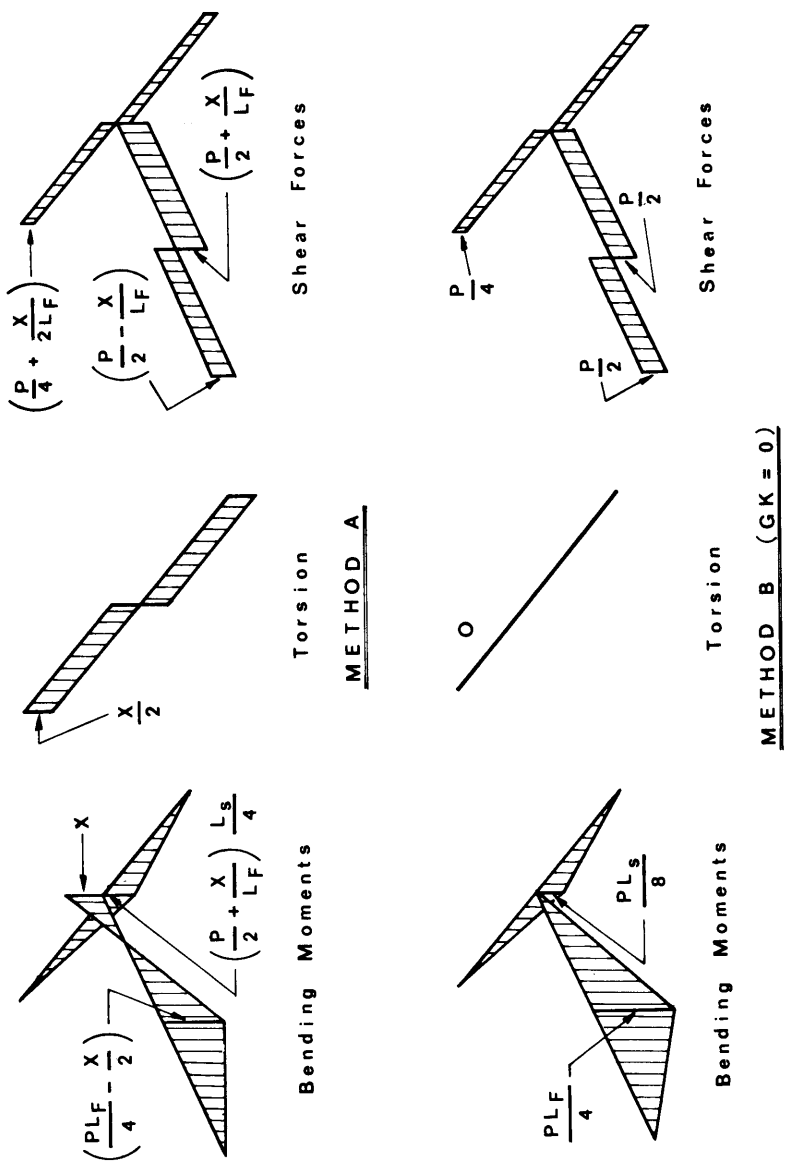


Fig. 11-3—Distribution of torsional and flexural moments

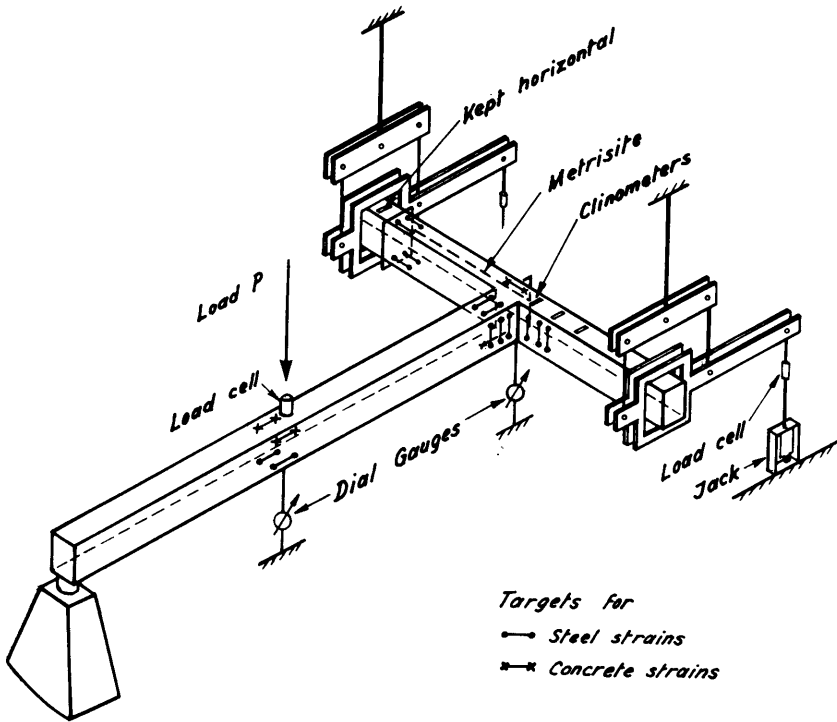


Fig. 11-4—Instrumentation of the specimen



Fig. 11-5—Test set-up

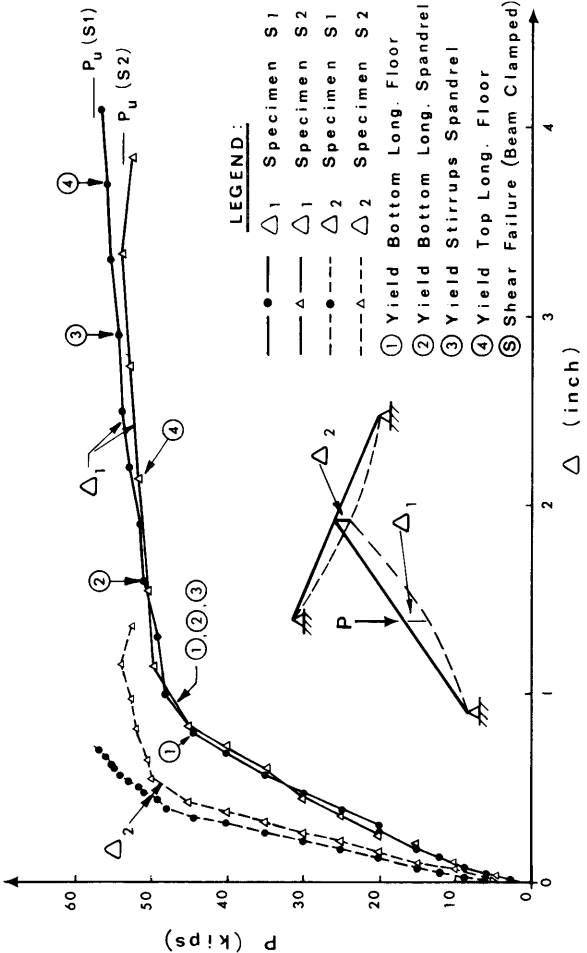


Fig. 11-6—Load—deflection for specimens S1 and S2

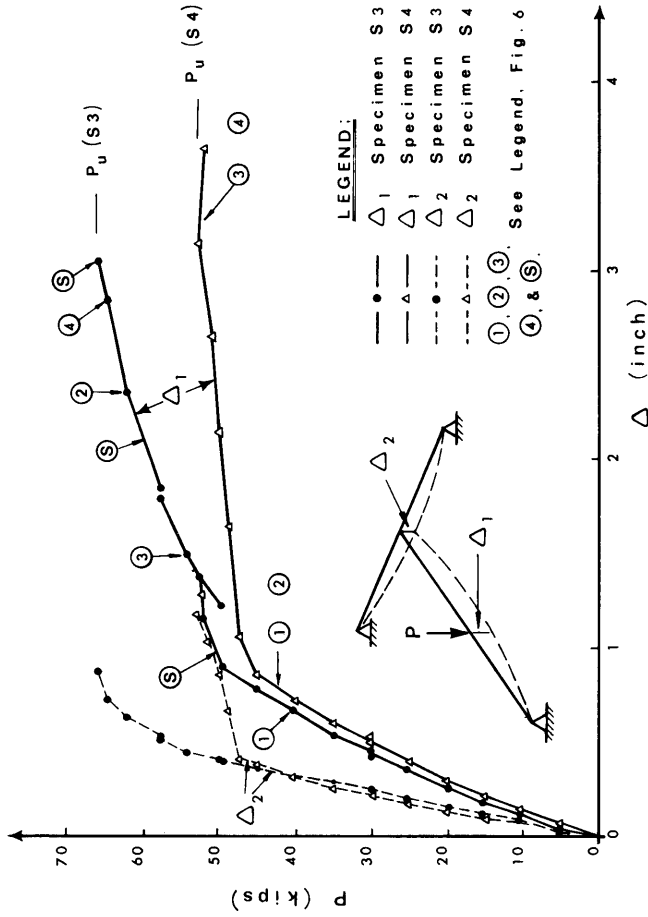


Fig. 11-7—Load—deflection for specimens S3 and S4

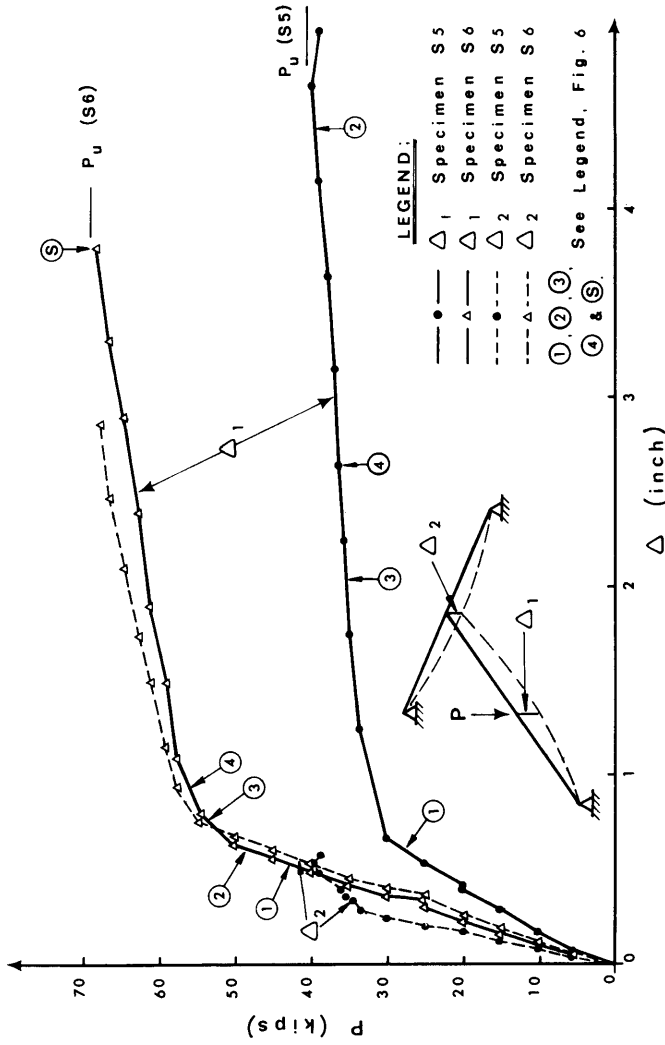


Fig. 11-8—Load—deflection for specimens S5 and S6

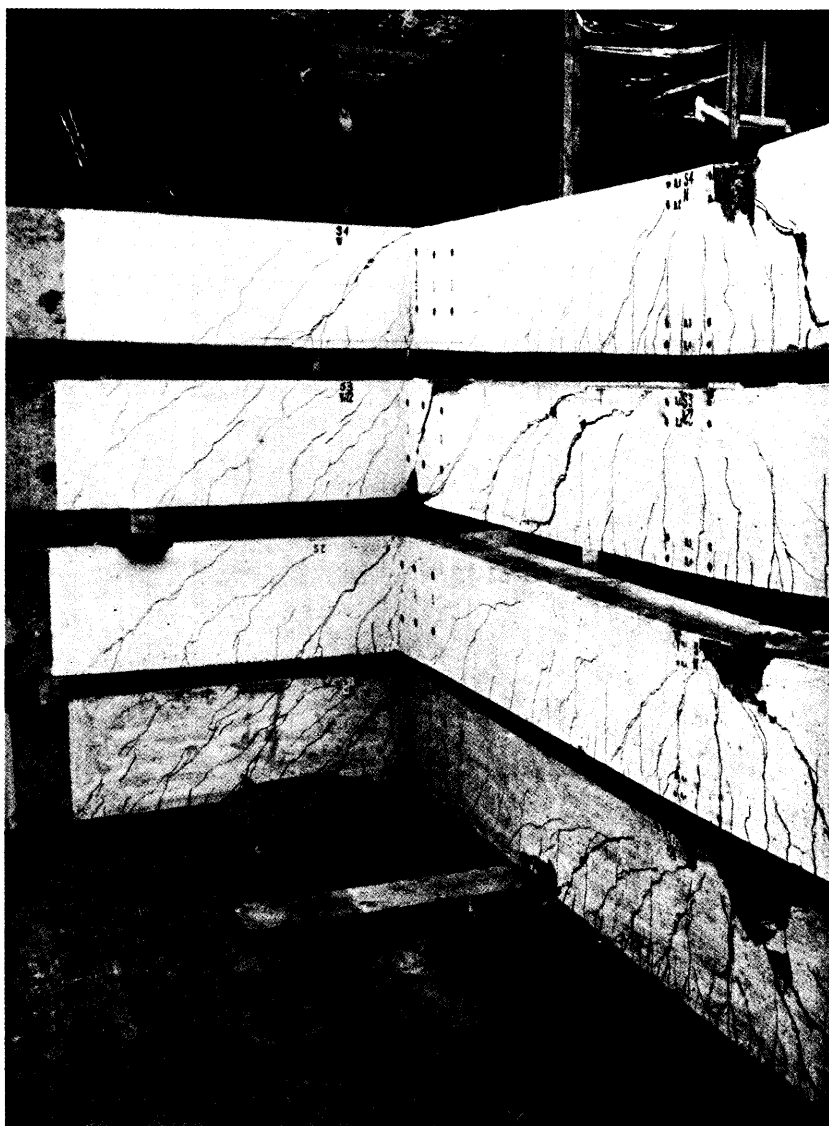
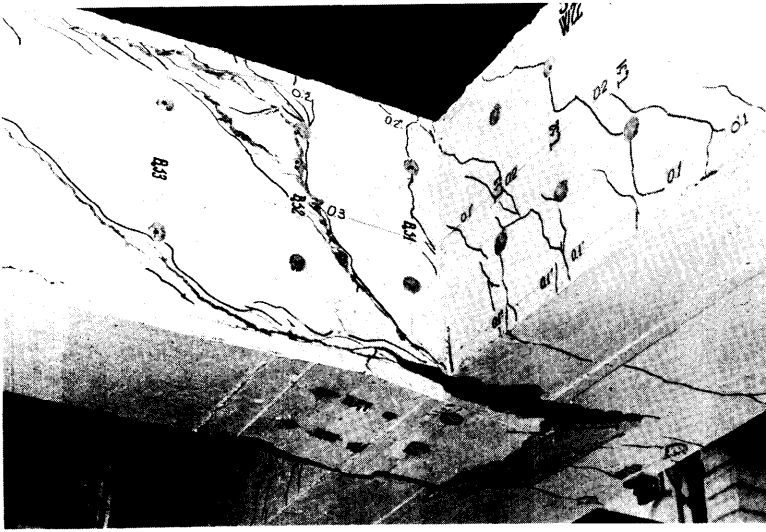
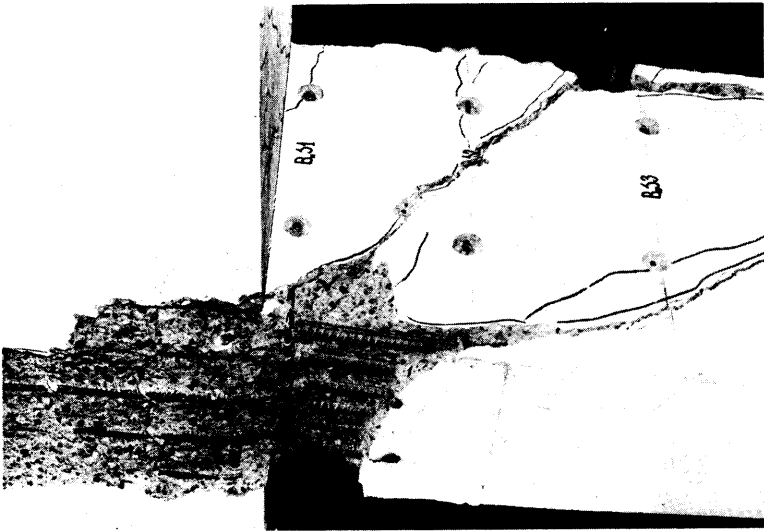


Fig. 11-9—Specimens S1, S2, S3, S4 after failure



Before Spalling



After Spalling

Fig. 11-10—Failure of the joint, specimen S3

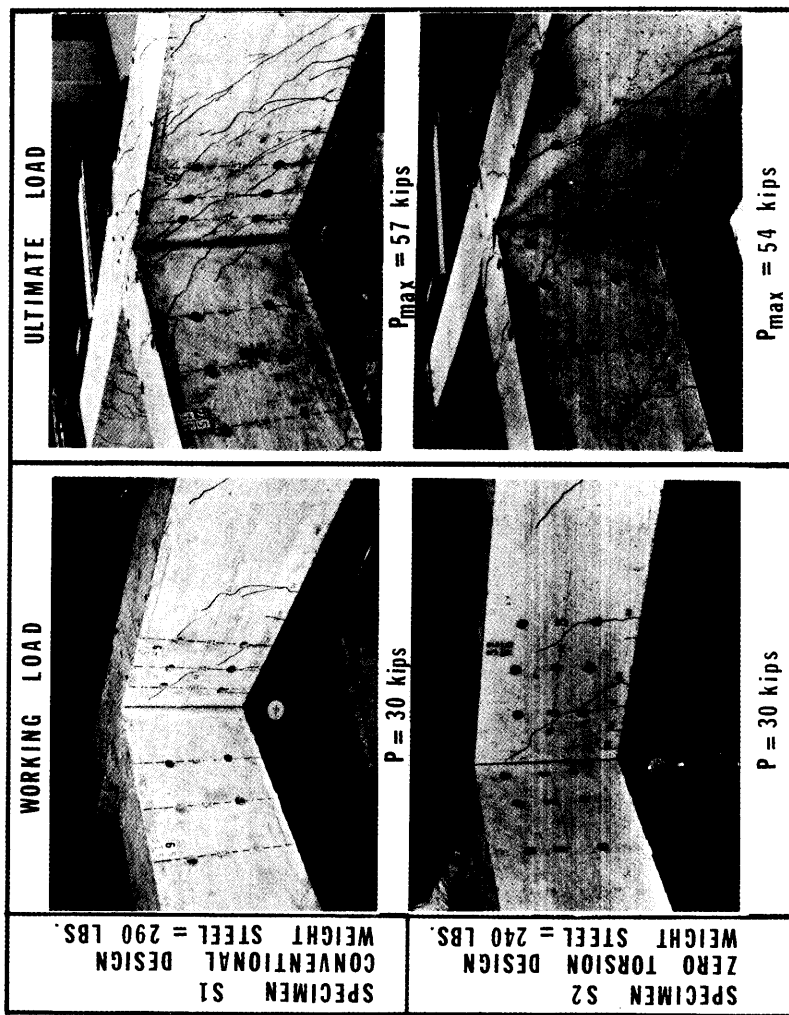


Fig. 11-11—Specimens S1 and S2 at service and ultimate load

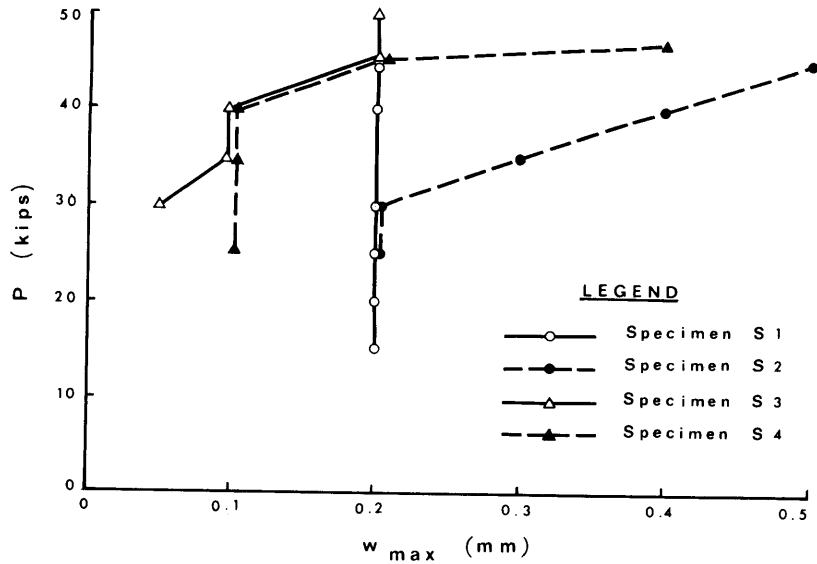


Fig. 11-12—Maximum crack widths at midheight of the spandrel beam

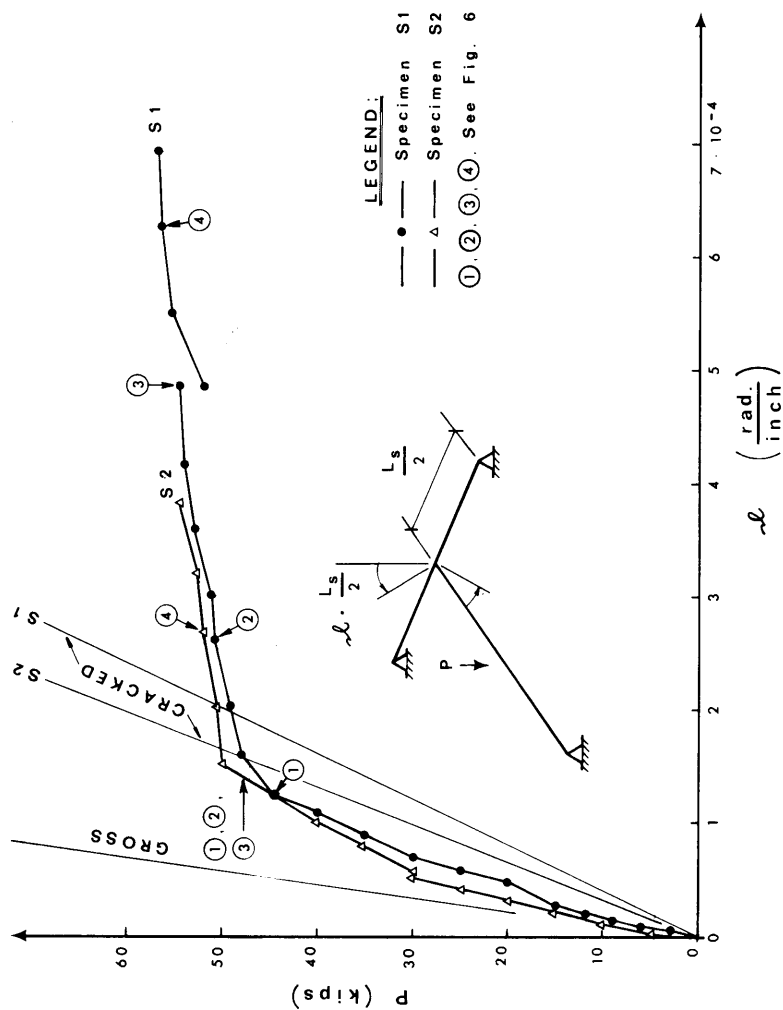


Fig. 11-13—Load—twist for specimens S1 and S2

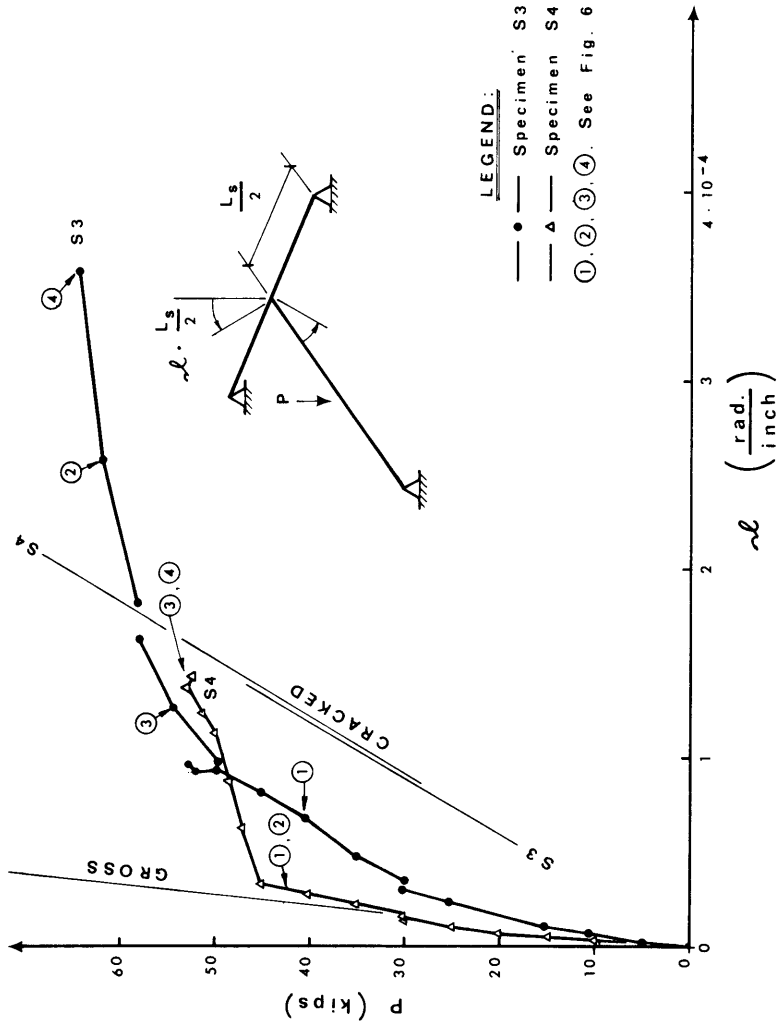


Fig. 11-14--Load--twist for specimens S3 and S4

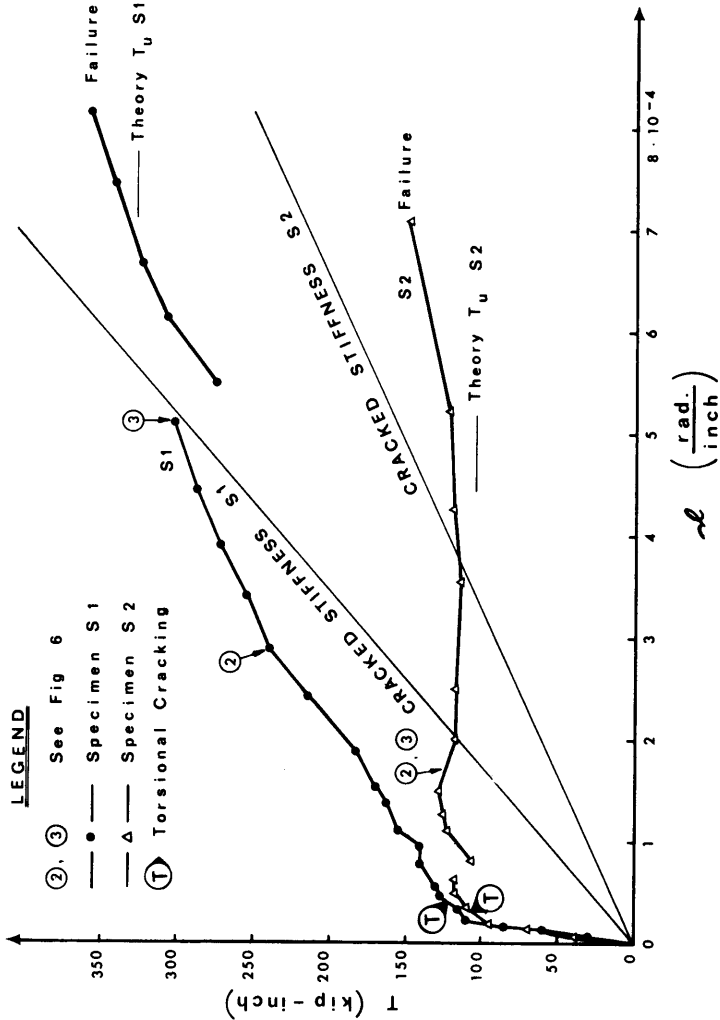


Fig. 11-15—Torque—twist for specimens S1 and S2

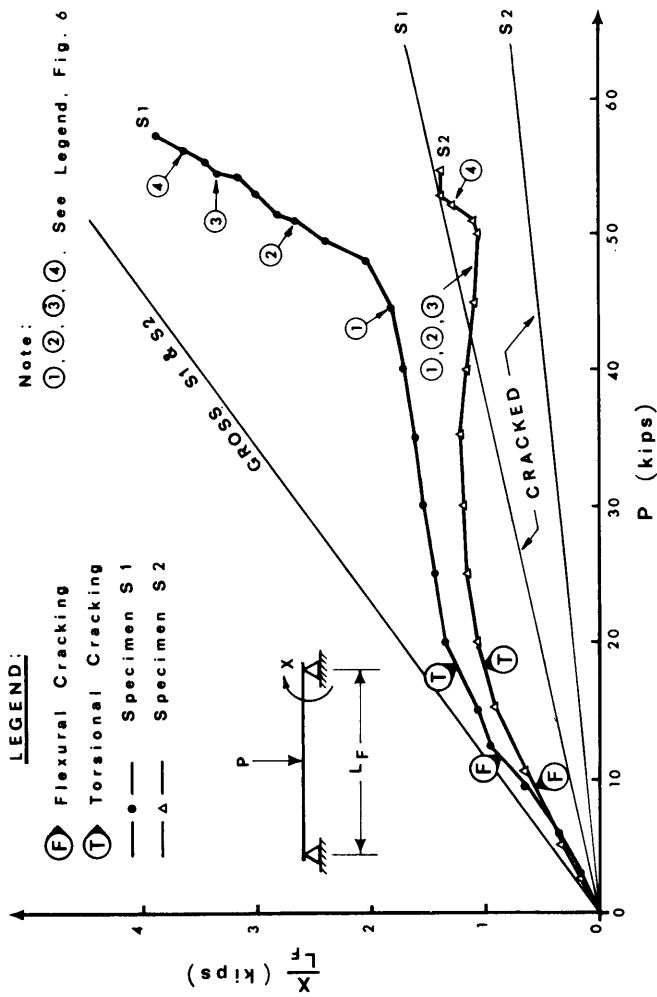


Fig. 11-16—Torque-load for specimens S1 and S2

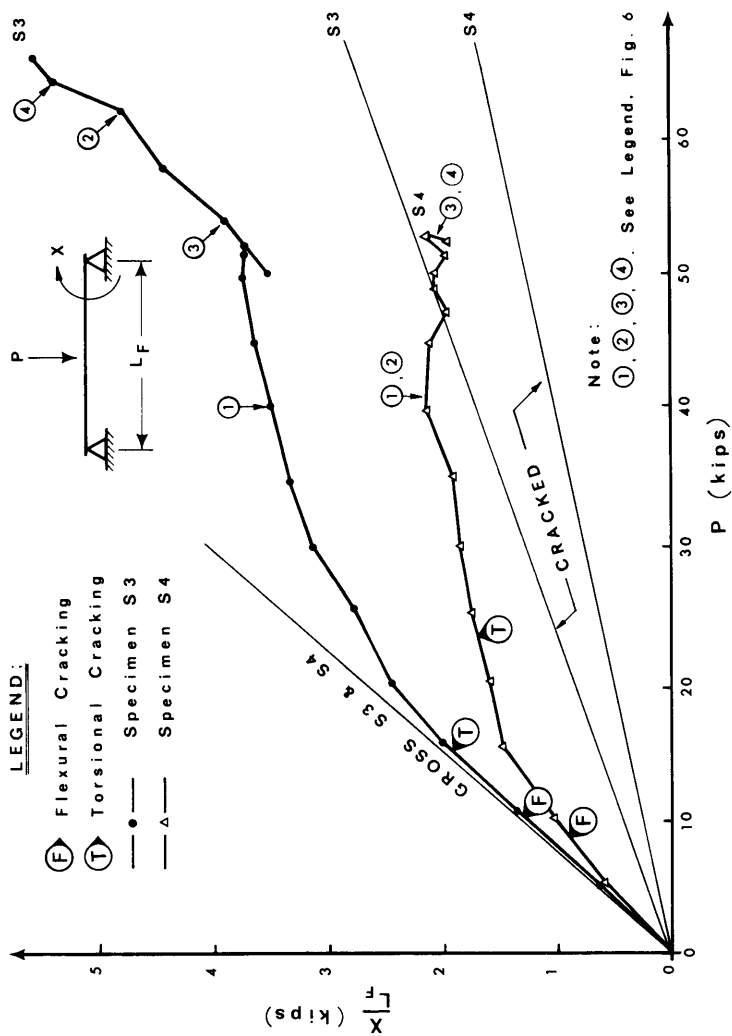


Fig. 11-17—Torque-load for specimens S3 and S4

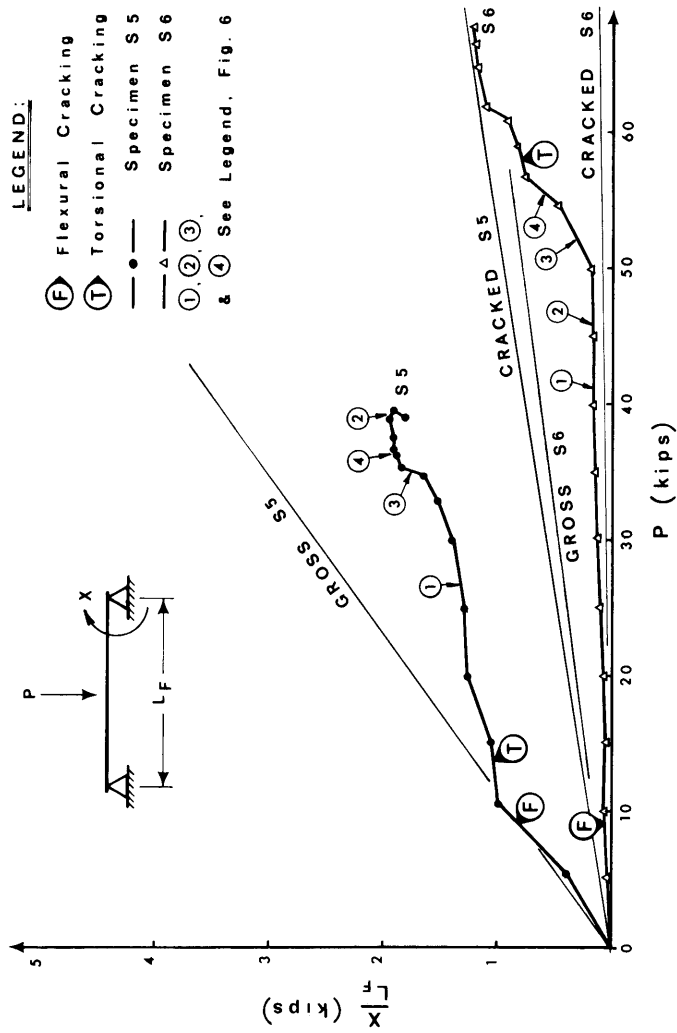


Fig. 11-18—Torque—load for specimens S5 and S6

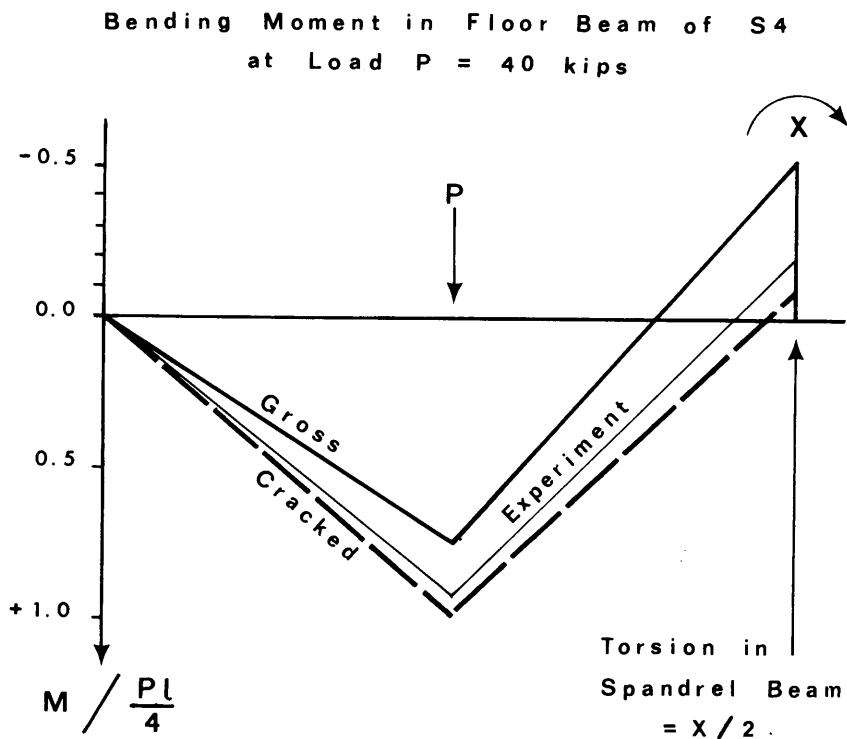


Fig. 11-19—Redistribution in specimen S4

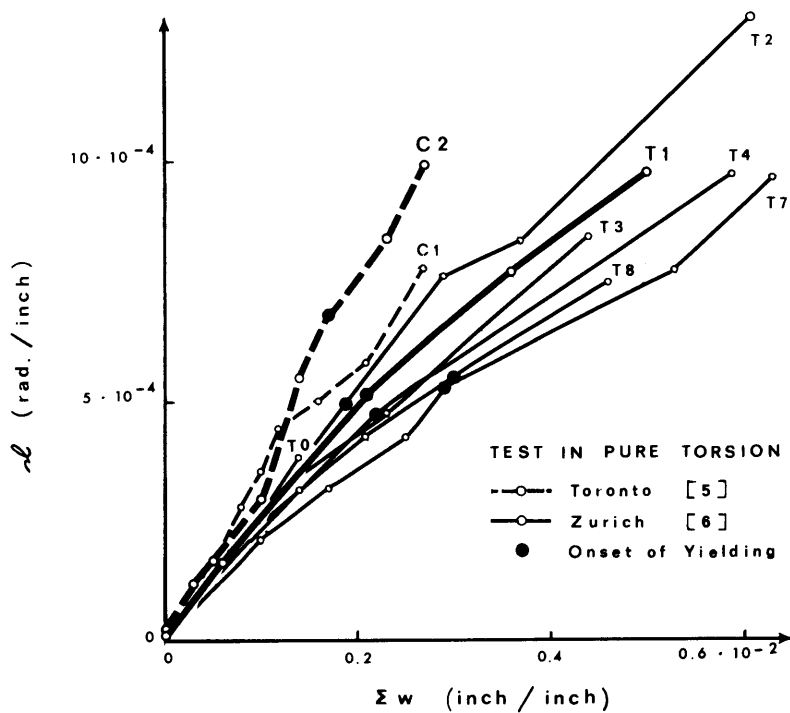


Fig. 11-20—Relationship between twist and the sum of crack widths^{5,6}

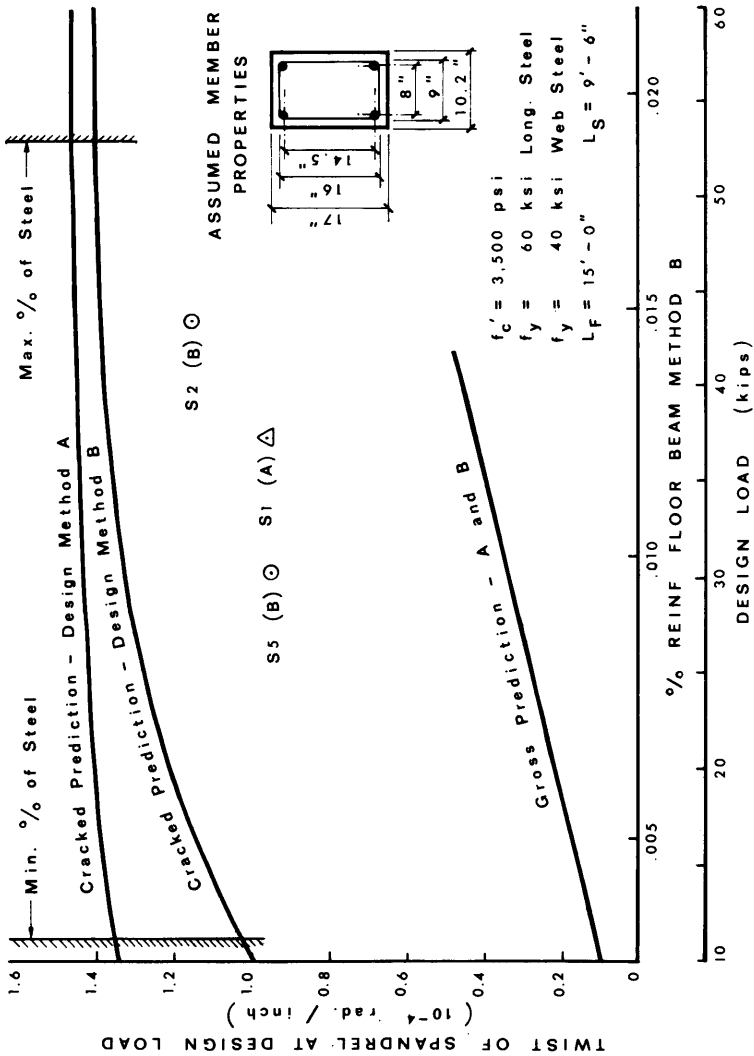


Fig. 11-21—Predicted twist of the spandrel beam for different percentages of reinforcement

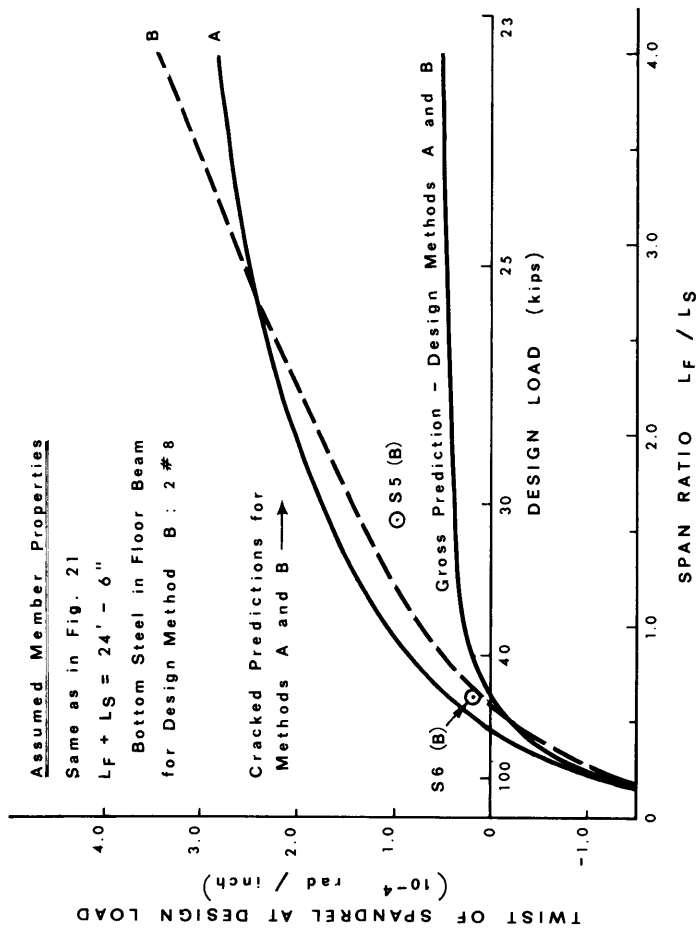


Fig. 11-22—Predicted twist of the spandrel beam for different span ratios

TABLE 11-1—TEST SPECIMENS

BEAM NO.	REINFORCEMENT FLOOR BEAM	REINFORCEMENT SPANDREL BEAM	DESIGN METHOD	DESIGN LOAD	PARAMETER	MATERIAL PROPERTIES
S 1	2 # 5 # 2 / 7.5" 2 # 8	2 # 5 # 3 / 4.25" 4 # 5	A ($E I_g, GK_g$)	37 kips	Basic Section $L_F = 15.0'$ $L_S = 9.5'$	Steel f_y (ksi) : # 2 : 45.0 # 4 : 42.5 # 5 : 58.5 Concrete f'_c (psi) : 3500 (Average of 120 cylinders)
S 2	2 # 3 # 2 / 7.5" 3 # 8	2 # 3 # 2 / 6" 5 # 4	B ($GK = 0$)	43 kips	Design Method	
S 3	4 # 5 # 2 / 7.5" 6 # 5	2 # 5 # 3 / 5.4" 5 # 5	A ($E I_g, GK_g$)	52 kips	Stiffness of Spandrel Beam	Steel f_y (ksi) : # 2 : 45.0 # 4 : 42.5 # 5 : 58.5 Concrete f'_c (psi) : 3500 (Average of 120 cylinders)
S 4	2 # 3 # 2 / 7.5" 3 # 8	2 # 3 # 2 / 6" 5 # 4	B ($GK = 0$)	43 kips	Design Method	
S 5	2 # 3 # 2 / 7.5" 2 # 8	2 # 3 # 2 / 6" 4 # 5	B ($GK = 0$)	30 kips	Percentage of Reinf.	Steel f_y (ksi) : # 2 : 45.0 # 4 : 42.5 # 5 : 58.5 Concrete f'_c (psi) : 3500 (Average of 120 cylinders)
S 6			B ($GK = 0$)	47 kips	Span Ratio $L_F = 9.5'$ $L_S = 15.0'$	

TABLE 11-2—GROSS AND CRACKED PREDICTIONS OF TORSION

Beam no.	Length ratio L_S/L_F	Gross stiffness ratios			Cracked stiffness ratios			Torsion in spandrel beam	
		$\left(\frac{EI_F}{EI_S}\right)^g$	$\left(\frac{EI_F}{GK_S}\right)^g$	$\left(\frac{EI_F}{EI_S}\right)^{cr}$	$\left(\frac{EI_F}{GK_S}\right)^{cr}$	$\frac{X}{PL_F}$ (gross)	$\frac{X}{PL_F}$ (cracked)		
S1	0.633	1.00	2.20	1.24	12.3	0.0868	0.0260		
S2	0.633	1.00	2.20	1.95	30.1	0.0868	0.0112		
S3	0.633	0.60	0.715	1.10	6.83	0.136	0.0420		
S4	0.633	0.60	0.715	1.78	12.1	0.136	0.0256		
S5	0.633	1.00	2.20	1.22	18.6	0.0868	0.0182		
S6	1.58	1.00	2.20	1.22	18.6	0.0162	0.00160		